

Published in final edited form as:

Eye Contact Lens. 2013 September ; 39(5): . doi:10.1097/ICL.0b013e31829fae00.

Entire thickness profiles of the epithelium and contact lens in vivo imaged with high speed and high resolution optical coherence tomography

Aizhu Tao, MD^{1,2}, Yilei Shao, MD^{1,2}, Hong Jiang, MD, PhD¹, Yufeng Ye, MD, PhD^{1,4}, Fan Lu, MD, OD², Meixiao Shen, PhD², Dexi Zhu, PhD², and Jianhua Wang, MD, PhD^{1,3}

¹Bascom Palmer Eye Institute, University of Miami, Miami, FL, USA

²School of Ophthalmology and Optometry, Wenzhou Medical College, Wenzhou, Zhejiang, China

³Electrical and Computer Engineering, University of Miami, Miami, FL, USA

⁴Hangzhou First People's Hospital, Hangzhou, China

Abstract

Purpose—To test the feasibility of measuring the entire thickness profiles of the epithelium and contact lens in vivo, using high speed and high resolution spectral domain optical coherence tomography (SD-OCT).

Methods—A custom-built, long scan depth SD-OCT was developed based on a CMOS camera and the axial resolution was about 5.1 μm in tissue. Five eyes of 5 subjects were imaged twice across the horizontal meridian before and while wearing one contact lens (CL). Semi-automatic measurement was done to yield the entire thickness profiles of the epithelium, total cornea, and contact lens after correcting for optical distortion.

Results—The full width and depth of the epithelium, ocular surface and contact lens were clearly visualized. The epithelial thickness (ET) at the center was $51.9 \pm 3.5 \mu\text{m}$, it remained at this thickness across the central 7 mm diameter and then increased at both temporal and nasal peripheries. The contact lens profile showed the thinnest point at the center with thickness of $100.3 \pm 4.9 \mu\text{m}$. The thickness increased towards the mid-periphery and then decreased at the edge.

Conclusions—This pilot study demonstrated the feasibility of using high speed CMOS-based OCT to evaluate the entire thickness profiles of the epithelium and contact lens in vivo. Further development will be needed to extend the scanning from 2D to 3D with a robust automatic image processing ability.

Corresponding Author: Jianhua Wang, MD, PhD, Mailing address: Bascom Palmer Eye Institute, University of Miami, Miller School of Medicine, 1638 NW 10th Avenue, McKnight Building - Room 202A, Miami, FL, 33136, USA. Tel: (305) 482-5010; Fax: (305) 482-5012; jwang3@med.miami.edu.

Publisher's Disclaimer: This is a PDF file of an unedited manuscript that has been accepted for publication. As a service to our customers we are providing this early version of the manuscript. The manuscript will undergo copyediting, typesetting, and review of the resulting proof before it is published in its final citable form. Please note that during the production process errors may be discovered which could affect the content, and all legal disclaimers that apply to the journal pertain.

Financial Disclosures

The authors have no proprietary interest in any materials or methods described within this article.

Contributions of the authors

Design of the study (AT, JW, YS); Conduct of the study, data collection, analysis and interpretation (AT, YS, HJ, JW, YY, FL, MS, DZ).

Keywords

cornea; epithelium; contact lens; optical coherence tomography

Introduction

The epithelium is critical in maintaining corneal power and corneal surface smoothness.¹ Previous studies have well documented the central epithelial thickness using different methods.²⁻⁴ However, thickness information for the central epithelium only may not be sufficient for some investigations or procedures, such as epithelial reshaping after orthokeratology and the epithelial response after contact lens (CL) wearing.^{5, 6} The accurate assessment of the total epithelium including the center and periphery, is useful for evaluating the severity of ocular surface disease.^{7, 8} Some researchers have divided the cornea into different zones and investigated the epithelial thickness at each region across the cornea.⁹⁻¹¹ Unlike the posterior segment of eye with some landmarks like retinal vessel branching, there are no similar marks currently for the cornea for stitching separated acquired images. Therefore, correctly registering the full width and depth of the epithelium using a montage of multiple images may be difficult. The exact location of the mid-periphery and periphery may be different for each subject, which may result in errors when comparing different subjects. Measuring the same location for serial visits was also impossible. Digital ultrasound has been reported to be used for imaging the epithelial map,^{8, 12} but it requires touching the eye and may not be suitable for the early postoperative period. Due to the lack of a large scan width, long scan depth and high resolution, imaging the entire epithelium from edge to edge using spectral-domain optical coherence tomography (SD-OCT) is difficult.

Different materials and designs of contact lenses may have unique fitting characteristics that will affect ocular comfort and ocular health. After insertion into the eye, a soft CL is reshaped according to the ocular shape, and therefore, the actual profile of a soft CL in vivo may be different from the profile in vitro. The clinical fitting performance of a soft CL is assessed mainly by slit-lamp biomicroscopy or quantified by video capture.^{13, 14} However, both methods give limited information on the interaction between the lens and ocular surface. Cui et al. and Shen et al. evaluated the movement of the CL and edge fitting using optical coherence tomography (OCT).^{15, 16} The diameter of a soft CL is approximately 14 mm, and the lenses cover the limbus on the eye. To image the whole CL in vivo, a scan width of at least 14 mm and scan depth of approximately 4 mm is needed. We previously reported an extended SD-OCT which is suitable for imaging the entire ocular surface, but the entire contact lens was only visualized after using the contrast enhancement agent.¹⁷ The relationship between the CL and ocular surface may change after using the enhancer. Improved from our previous system, we recently developed a long scan depth SD-OCT based on a complementary metal oxide semiconductor (CMOS), the aim of this study was to demonstrate the feasibility of measuring the entire thickness profiles of the epithelium and CL in vivo using this high speed, high resolution OCT.

Subjects and Methods

Subjects

The study was approved by the University of Miami review board, and written informed consent was obtained from each subject. All subjects were treated in accordance with the tenets of the Declaration of Helsinki. Each subject was free of ocular diseases or systemic diseases.

CMOS-based OCT

To detect the entire profiles of the epithelium and CL, a custom-built SD-OCT was developed with a high acquisition speed of up to 70,000 A-lines per second. A superluminescent diode light source (InPhenix, IPSDD0808, Livermore, CA, USA) with a full width at half maximum bandwidths of 50 nm, centered at 840 nm, was used to provide low coherence light. The light was coupled with a fiber-based Michelson interferometer after passing through a fiber-pigtailed isolator. It split the light into the reference and sample arms by a 50:50 fiber coupler. A telecentric light delivery system that was driven by an X-Y galvanometer scanner design and video viewing system were co-axially aligned and mounted with a modified slit-lamp. The power of the incident light was 1.307 mW, which was a safe level of exposure to the eye.¹⁸ A spectrometer based on a CMOS camera (Basler sprint spL4096-140k; 4096 pixels, Basler AG, Germany), an achromatic imaging lens ($f = 210$ mm), and a 1,800 line/mm transmission grating (Wasatch Photonics, Logan, UT) was used to detect the reference and sample light. The images captured by the camera were delivered to a computer workstation for display and processing. Software was custom developed in Labview (National Instrument, Austin, TX) to control the instrument during measurements and also to provide data acquisition. The calculated spectral resolution of the spectrometer was 0.017 nm,¹⁹ corresponding to a scan depth of 10.4 mm in air. The measured axial resolution of the OCT system for 4096 pixels was 7.0 μm in air and 5.1 μm in tissue, assuming the refractive index was 1.38. The ideal axial resolution determined by the light source in air is 6.3 μm .²⁰

Experimental procedure and image analysis

In 5 subjects (4 males and 1 female, mean age: 35.0 ± 9.8 years), 5 eyes were imaged twice across the horizontal meridian before and while wearing one CL (PureVision, Bausch & Lomb, Rochester, NY). The base curve of the CL was 8.3 mm with a spherical diopter (D) of -3.00 D, and had been on the eye for 5 minutes at time of imaging. During imaging, the subjects were asked to look straight ahead to an external central target. The live image was aligned in both the X and Y meridians,²¹ and acquisition occurred when the light was at the corneal apex in both directions. Horizontal scan widths of 12.82 mm and 18.00 mm were set to image the epithelium and ocular surface in a single B scan, respectively. The acquisition rate was set at 35,000 A-lines per second, and the zero delay plane was placed in front of the cornea. The scan width was set to 16.32 mm for the CL. The acquisition rate was set at 10,000 A-lines per second with the zero delay near the depth of the iris for the CL. The image size was 4096 pixels \times 4096 pixels.

Custom software (J-OCT-1, Ver 1.0) was used for image processing as described in a previous study.²² Briefly, a small square “locked on” to the nearest peak for the cursor to locate points of interest on the surface; when several points were entered along the surface, the software curve fitted an appropriate radius between the points to describe the intermediate points. The boundaries of each layer were semi-automatically detected by this software. After correcting for optical distortion,²³ refractive indices of 1.401 and 1.389 were used to calculate the entire thickness profiles of the epithelium and total cornea, respectively.^{24, 25} The refractive index of 1.426 according to the manufacturer was used to yield the thickness profile of the CL.

To compare the image quality with that in previous study, each subject was also imaged with the same custom-built extended scan depth OCT (EX-OCT) that had been used in our earlier study.¹⁷ In the spectrometer, a charge-coupled device (CCD) camera (Aviiva-SM2010, 2,048 pixels; Atmel, e2v Inc., Elmsford, NY) was used. The measured axial resolution of this system was 10.4 μm in air and the scan depth was 7.3 mm in air. The acquisition rate of the UL-OCT was set at 12,000 A lines per second. The same scan widths

were used for the epithelium, cornea and CL images. The image size was 2048 pixels \times 2048 pixels. The data were presented as the means \pm standard deviation (SD). The repeatability of each thickness layer was expressed as a SD of the difference between two measurements for the same subject.

Results

The full width and depth of the epithelium and ocular surface were clearly visualized with CMOS-based OCT system (Fig. 1b). The mean epithelial thickness (ET) at the center was $51.9 \pm 3.5 \mu\text{m}$, and it remained at this thickness across the central approximately 7 mm diameter and then increased at both the temporal and nasal peripheries (Table 1, Fig. 2). The overall repeatability of ET was $2.5 \pm 1.0 \mu\text{m}$. The repeatability of ET at the center was better than that in the peripheral zone (Table 2). Bowman's layer at the center was clearly visualized by this OCT system (Fig. 1c). In contrast, using EX-OCT, only the center and mid-periphery of the epithelium were visualized, the periphery of the epithelium and Bowman's layer were not clear (Fig. 1e). Using EX-OCT, the visualized epithelial diameter ranged from 5.0 mm to 9.3 mm among five subjects, the mean epithelial thickness (ET) at the center was $49.8 \pm 4.5 \mu\text{m}$, and the overall repeatability of ET was $10.5 \pm 13.8 \mu\text{m}$. The total corneal thickness (CT) increased gradually from the center to the periphery (Table 1, Fig. 2, Fig.3). The repeatability of the CT was $3.9 \mu\text{m}$ at the center and $19.0 \mu\text{m}$ at the periphery using CMOS-based OCT. The repeatability of the CT was $2.2 \mu\text{m}$ at the center and $15.7 \mu\text{m}$ at the periphery using EX-OCT.

The entire CL from edge to edge in vivo was clearly visualized using CMOS-based OCT system (Fig. 3a). The mean CL profile showed the thinnest point at the center was $100.3 \pm 4.9 \mu\text{m}$. The thickness increased towards the mid-periphery and then decreased at the edge (Table 1, Fig. 2). Overall, the repeatability was $7.2 \pm 3.1 \mu\text{m}$. In contrast, the edge of the CL was not available in the EX-OCT image (Fig. 3c). Using EX-OCT, the visualized CL diameter ranged from 5.7 mm to 8.9 mm among five subjects, the mean CL thickness at the center was $97.1 \pm 8.0 \mu\text{m}$. Overall, the repeatability of visualized CL was $12.1 \pm 17.2 \mu\text{m}$.

Discussion

Theoretical axial resolution of the OCT system is determined by the central wavelength and spectral width of the light source.²⁰ The same light source was used for CMOS-based OCT and EX-OCT in the present study, and thus the theoretical axial resolution is the same (6.3 μm in air). In fact, CMOS has the full spectrum projected on the 4096 camera pixels, whereas EX-OCT truncates the spectrum projected on the 2048 camera pixels, which causes the axial resolution and sensitivity to decrease together. As a consequence, the measured axial resolutions of CMOS-based OCT and EX-OCT were 7.0 μm and 10.4 μm in air, respectively.²¹ Bowman's layer was clearly visualized with CMOS-based OCT but not very clear in the image obtained by EX-OCT. The visualization of Bowman's layer may indicate that the image is high quality, which is correlated with the axial resolution. Grulkowski et al. suggested that CMOS can improve the sensitivity roll-off performance, which was in agreement with the present study.²⁶

The sensitivity drop is an inevitable defect in SD-OCT, with the sensitivity and resolution decreasing as the scan depth increases. Below the half image depth, it was difficult to visualize the epithelium. Ge et al. developed an automated image processing algorithm to detect the central epithelium thickness and found that the algorithm failed for images located below the middle image depth.²² Although the whole scan depth of this system was 10.4 mm, only half image depth was needed for imaging the entire epithelium, therefore, the region with the best signal has been used. To achieve ultra-high resolution for the entire

epithelial images, a shallow scan depth OCT system with a broadband light source will be developed in the future. Some methods, such as complex conjugate image removal and switchable reference arm (overlapping two images when the zero-delay line was alternatively placed on the top or the bottom of the images), may also improve the signal-to-noise ratio (SNR) for the entire epithelium and CL.^{26, 27}

Although the human eye may move during OCT imaging, high speed minimizes the motion artifacts, and thus the speed is important in the OCT system for good repeatability. CMOS-based OCT has a high speed that allows the image to be obtained in very short time. For EX-OCT, at least 83 ms are required to obtain one epithelial image consisting of 2048 pixels, and the axial motion of the eye can be 25 μm during this period.²⁸ However, only 58 ms are required to obtain one B-scan image of the epithelium consisting of 4096 pixels in CMOS-based OCT. The speed will be critical for 3D scan in future studies.

Good repeatability is a key point for precise measurement and reliably monitoring in normal and diseased conditions. To validate our new system with the improved speed and more camera pixels for sensing the full bandwidth of the light source, we compared the image quality and repeatability between two OCT systems. The repeatability of total corneal thickness was similar with two OCT systems, whereas the repeatability of epithelial thickness and contact lens thickness were better with the CMOS-based OCT than the EX-OCT. Ge et al. evaluated the repeatability of epithelial thickness among three OCT devices with different axial resolutions and found that the axial resolution may affect the repeatability of the epithelial thickness measurement.²⁹ High resolution might increase the capability to determine the layer boundaries, which is in agreement with the present study. The repeatability of epithelial and total corneal thickness in this study was slightly larger than our previous study,²⁹ which may be due to small sample size in the present study. The repeatability at the periphery was greater than that at the center, the main possible reason was the signal-to-noise ratio (SNR) gradually decreased as the image depth increased. From the zero-delay plane (near the corneal center) to the limbal-scleral regions, the SNR decreased by 16 dB in CMOS-based OCT (3.5 mm depth). The decreased SNR caused the decrease of boundary contrast, which may decrease the precision in the detection of the location of the front and back surfaces, thus impacting the precision of the measurement.²¹ The slightly poor repeatability of CL at the periphery may be explained by the lens decentration during measurement, further improvement with 3D scan may solve the problem.

This study demonstrated the use of a high resolution CMOS-based SD-OCT for the measurement of the thickness profile of the entire epithelium in one image. Using EX-OCT, the periphery of epithelium was not very clear and only partial width of the epithelial thickness was analyzed with EX-OCT. Grulkowski et al. represented an image of entire cornea and magnified to show the central epithelium.²⁶ We are not sure if they can outline the entire epithelium since they did not mention it. In the present study, the entire epithelium was visualized for each subject. The epithelial thickness at the center in this study was $51.9 \pm 3.5 \mu\text{m}$, which is within the range of previous studies.^{3, 9} It remained at this thickness across the central approximately 7 mm diameter and then increased at both the temporal and nasal peripheries. This uneven trend is in agreement with Reinstain et al.'s study³⁰ but different from Wang et al.'s study.³¹ Different resolutions and locations may explain this trend. Schmoll et al. and Li et al. have measured the central epithelium with semi-automatic or automatic methods,^{4, 32} and in the present study, we demonstrated the capability to measure the entire epithelium using a semi-automatic method. Further development will be needed to extend the scanning from 2D to 3D with a robust automatic image processing ability.

Most soft contact lenses cover the limbus onto the sclera by approximately 1 mm all around, and the lenses need to have the greatest flexibility to fit the ocular surface at the limbus. The objective evaluation of the full range CL fitting may help the understanding of the ocular surface shape and its interaction with the soft CL in vivo. Grulkowski et al. presented an image of the soft CL on the eye containing 15,000 A-scans.²⁶ In the present study, we demonstrated the feasibility of measuring the entire thickness profile of the CL in vivo, containing 4096 A-scans, using OCT, which means less time to acquire one CL image than the former study. Shen et al.¹⁷ imaged the entire CL using EX-OCT with a lubricant eye drop, the relationship between the CL and ocular surface may change after using such an enhancement. In contrast, we imaged the CL in the natural state, and this method may more accurately reflect the actual relationship between the CL and ocular surface. With this high resolution CMOS-based OCT, imaging the entire epithelium and cornea for studying the corneal response to CL wear without removing the lens is now possible. The technology for evaluating the entire CL thickness profile demonstrated in the present study may open a new era for improving the design and fitting of the lens. The relationships between the ocular surface and overall fitting characteristics of different types of contact lenses in vivo may be explored in further studies.

In conclusion, this pilot study demonstrated the feasibility of using high speed CMOS-based OCT to evaluate the entire thickness profiles of the epithelium and CL in vivo. This method may be applied in the field of CL design and fitting. Further work will involve the development of the automatic segmentation of the entire epithelium and CL in three dimensional maps.

Acknowledgments

Funding / Support

This study was supported by research grants from the NIH 1R21EY021336, NIH Center Grant P30 EY014801 and Research to Prevent Blindness (RPB). Visiting scholar activity (YLS) was supported by research grants from the Affiliated Eye Hospital of Wenzhou Medical College (YNZD201004).

Statement about conformity

The research review board of University of Miami approved this study.

References

1. Simon G, Ren Q, Kervick GN, et al. Optics of the corneal epithelium. *Refract. Corneal Surg.* 1993; 9:42–50. [PubMed: 8481372]
2. Hutchings N, Simpson TL, Hyun C, et al. Swelling of the human cornea revealed by high-speed, ultrahigh-resolution optical coherence tomography. *Invest Ophthalmol. Vis. Sci.* 2010; 51:4579–4584. [PubMed: 20435597]
3. Sin S, Simpson TL. The repeatability of corneal and corneal epithelial thickness measurements using optical coherence tomography. *Optom. Vis. Sci.* 2006; 83:360–365. [PubMed: 16772894]
4. Li Y, Tan O, Brass R, et al. Corneal epithelial thickness mapping by fourier-domain optical coherence tomography in normal and keratoconic eyes. *Ophthalmology.* 2012; 119:2425–2433. [PubMed: 22917888]
5. Reinstein DZ, Gobbe M, Archer TJ, et al. Epithelial, stromal, and corneal pachymetry changes during orthokeratology. *Optom. Vis. Sci.* 2009; 86:E1006–E1014. [PubMed: 19584769]
6. Wang J, Fonn D TL, Simpson. Topographical thickness of the epithelium and total cornea after hydrogel and PMMA contact lens wear with eye closure. *Invest Ophthalmol Vis. Sci.* 2003; 44:1070–1074. [PubMed: 12601031]

7. Francoz M, Karamoko I, Baudouin C, et al. Ocular surface epithelial thickness evaluation with spectral-domain optical coherence tomography. *Invest Ophthalmol. Vis. Sci.* 2011; 52:9116–9123. [PubMed: 22025572]
8. Kanellopoulos AJ, Aslanides IM, Asimellis G. Correlation between epithelial thickness in normal corneas, untreated ectatic corneas, and ectatic corneas previously treated with CXL; is overall epithelial thickness a very early ectasia prognostic factor? *Clin. Ophthalmol.* 2012; 6:789–800. [PubMed: 22701079]
9. Tao A, Wang J, Chen Q, et al. Topographic thickness of Bowman's layer determined by ultra-high resolution spectral domain-optical coherence tomography. *Invest Ophthalmol. Vis. Sci.* 2011; 52:3901–3907. [PubMed: 21460260]
10. Feng Y, Simpson TL. Corneal, limbal, and conjunctival epithelial thickness from optical coherence tomography. *Optom. Vis. Sci.* 2008; 85:E880–E883. [PubMed: 18772715]
11. Du C, Wang J, Cui L, et al. Vertical and horizontal corneal epithelial thickness profiles determined by ultrahigh resolution optical coherence tomography. *Cornea.* 2012; 31:1036–1043. [PubMed: 22357393]
12. Reinstein DZ, Archer TJ, Gobbe M. Epithelial thickness up to 26 years after radial keratotomy: three-dimensional display with Artemis very high-frequency digital ultrasound. *J. Refract. Surg.* 2011; 27:618–624. [PubMed: 21323239]
13. Golding TR, Bruce AS, Gaterell LL, et al. Soft lens movement: effect if blink rate on lens settling. *Acta Ophthalmol Scand.* 1995; 73:506–511. [PubMed: 9019373]
14. Brennan NA, Lindsay RG, McCraw K, et al. Soft lens movement: temporal characteristics. *Optom. Vis. Sci.* 1994; 71:359–363. [PubMed: 8090437]
15. Cui L, Shen M, Wang MR, et al. Micrometer-scale contact lens movements imaged by ultrahigh-resolution optical coherence tomography. *Am. J. Ophthalmol.* 2012; 153:275–283. [PubMed: 21920493]
16. Shen M, Cui L, Riley C, et al. Characterization of soft contact lens edge fitting using ultra-high resolution and ultra-long scan depth optical coherence tomography. *Invest Ophthalmol. Vis. Sci.* 2011; 52:4091–4097. [PubMed: 21372023]
17. Shen M, Wang MR, Wang J, et al. Entire contact lens imaged in vivo and in vitro with spectral domain optical coherence tomography. *Eye Contact Lens.* 2010; 36:73–76. [PubMed: 20093938]
18. American National Standards Institute. Laser Institute of America. Orlando, FL: 2000. American National Standard for Safe Use of Lasers; p. 45-49. ANSI Z 136.1-2000
19. J, Ai; Wang, LV. Spectral-domain optical coherence tomography: Removal of autocorrelation using an optical switch. *Appl. Phys. Lett.* 2006; 88:111115.
20. Wojtkowski M, Srinivasan V, Ko T, et al. Ultrahigh-resolution, high-speed, Fourier domain optical coherence tomography and methods for dispersion compensation. *Opt. Express.* 2004; 12:2404–2422. [PubMed: 19475077]
21. Shen M, Cui L, Li M, et al. Extended scan depth optical coherence tomography for evaluating ocular surface shape. *J. Biomed. Opt.* 2011; 16:056007. [PubMed: 21639575]
22. Ge L, Shen M, Tao A, et al. Automatic segmentation of the central epithelium imaged with three optical coherence tomography devices. *Eye Contact Lens.* 2012; 38:150–157. [PubMed: 22415151]
23. Yuan Y, Chen F, Shen M, et al. Repeated measurements of the anterior segment during accommodation using long scan depth optical coherence tomography. *Eye Contact Lens.* 2012; 38:102–108. [PubMed: 22223160]
24. Lin RC, Shure MA, Rollins AM, et al. Group index of the human cornea at 1.3-microm wavelength obtained in vitro by optical coherence domain reflectometry. *Opt. Lett.* 2004; 29:83–85. [PubMed: 14719668]
25. Patel S, Marshall J, Fitzke FW III. Refractive index of the human corneal epithelium and stroma. *J. Refract. Surg.* 1995; 11:100–105. [PubMed: 7634138]
26. Grulkowski I, Gora M, Szkulmowski M, et al. Anterior segment imaging with Spectral OCT system using a high-speed CMOS camera. *Opt. Express.* 2009; 17:4842–4858. [PubMed: 19293916]

27. Du C, Shen M, Li M, et al. Anterior segment biometry during accommodation imaged with ultralong scan depth optical coherence tomography. *Ophthalmology*. 2012; 119:2479–2485. [PubMed: 22902211]
28. Pircher M, Baumann B, Gotzinger E, et al. Simultaneous SLO/OCT imaging of the human retina with axial eye motion correction. *Opt. Express*. 2007; 15:16922–16932. [PubMed: 19550983]
29. Ge L, Yuan Y, Shen M, et al. The role of axial resolution of optical coherence tomography on the measurement of corneal and epithelial thicknesses. *Invest Ophthalmol. Vis. Sci*. 2013; 54:746–755. [PubMed: 23139281]
30. Reinstein DZ, Archer TJ, Gobbe M, et al. Epithelial thickness in the normal cornea: three-dimensional display with Artemis very high-frequency digital ultrasound. *J. Refract. Surg*. 2008; 24:571–581. [PubMed: 18581782]
31. Wang J, Thomas J, Cox I, et al. Noncontact measurements of central corneal epithelial and flap thickness after laser in situ keratomileusis. *Invest Ophthalmol. Vis. Sci*. 2004; 45:1812–1816. [PubMed: 15161844]
32. Schmoll T, Unterhuber A, Kolbitsch C, et al. Precise thickness measurements of Bowman's layer, epithelium, and tear film. *Optom. Vis. Sci*. 2012; 89:E795–E802. [PubMed: 22488267]

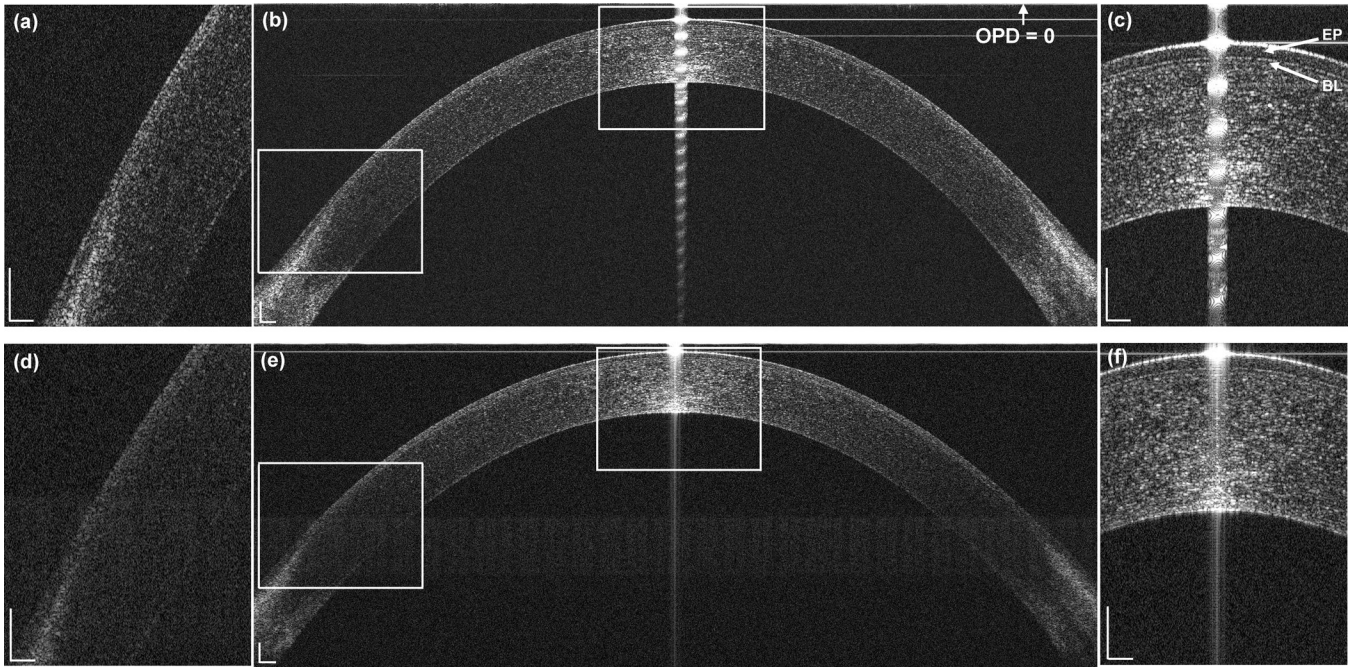


Figure 1. Representative CMOS-based OCT (b) and EX-OCT (e) images of the epithelium and magnified images at the apex (c, f) and limbus (a, d)
 The zero delay line (optical path difference $OPD = 0$) is indicated. (b) The entire epithelium from edge to edge was clearly visualized by CMOS-based OCT. (e) The periphery of the epithelium was not very clear in the EX-OCT system. EP: epithelium; BL: Bowman's layer. Bars = 250 μm .

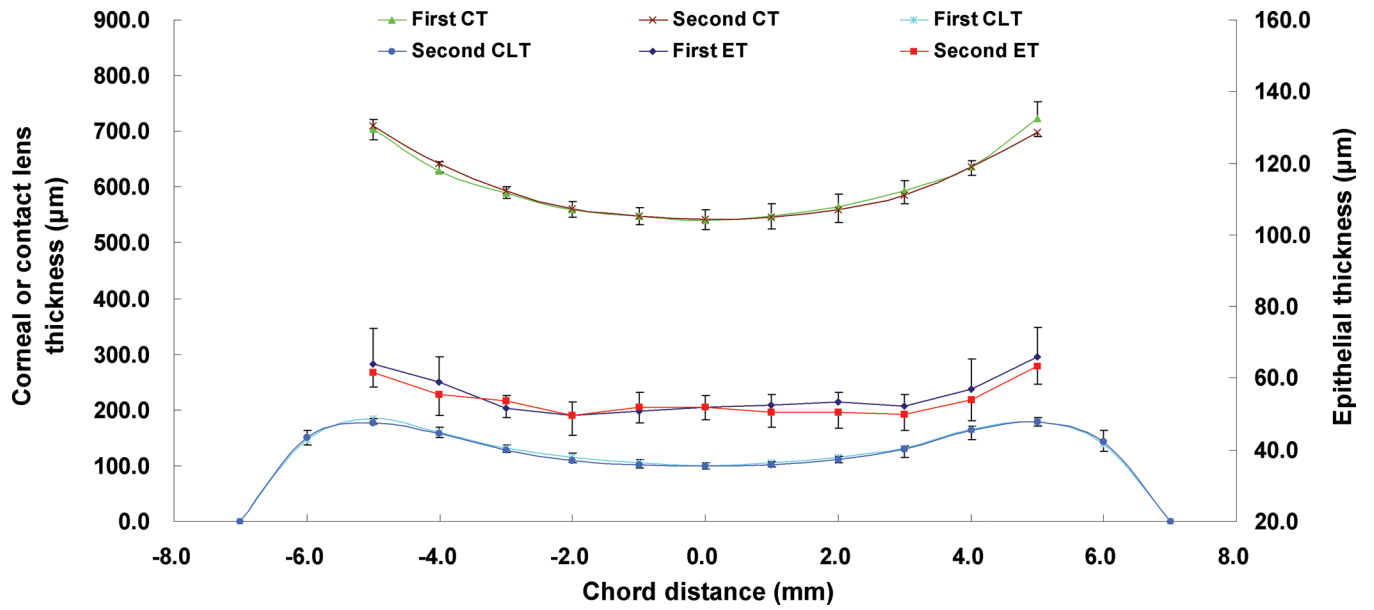


Figure 2. Replicate thickness profiles of the total cornea (CT), contact lens (CLT), and epithelium (ET) for five eyes of five subjects
 The repeatability of the overall CT, CLT, and ET was good. First represents the first measurement, and second represents the second measurement.

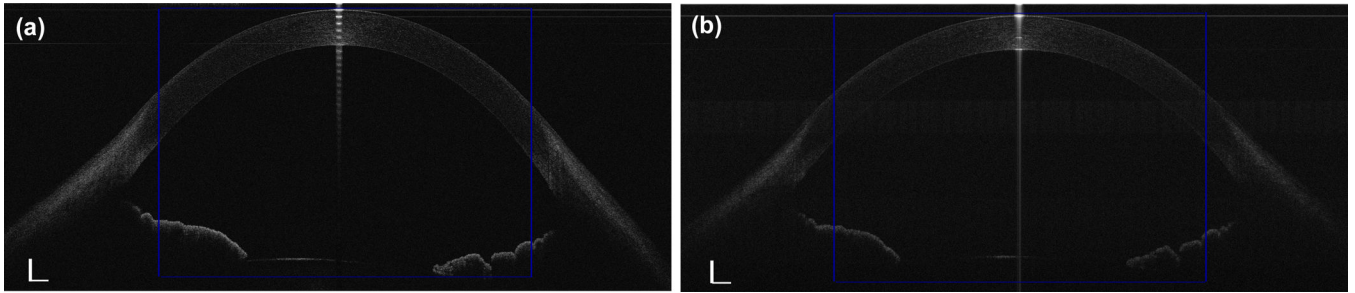


Figure 3. Representative CMOS-based OCT (a) and EX-OCT (b) images of the total cornea
A 10.00 mm chord distance centered on the cornea apex, were selected for data analysis.
Bars = 500 μm .

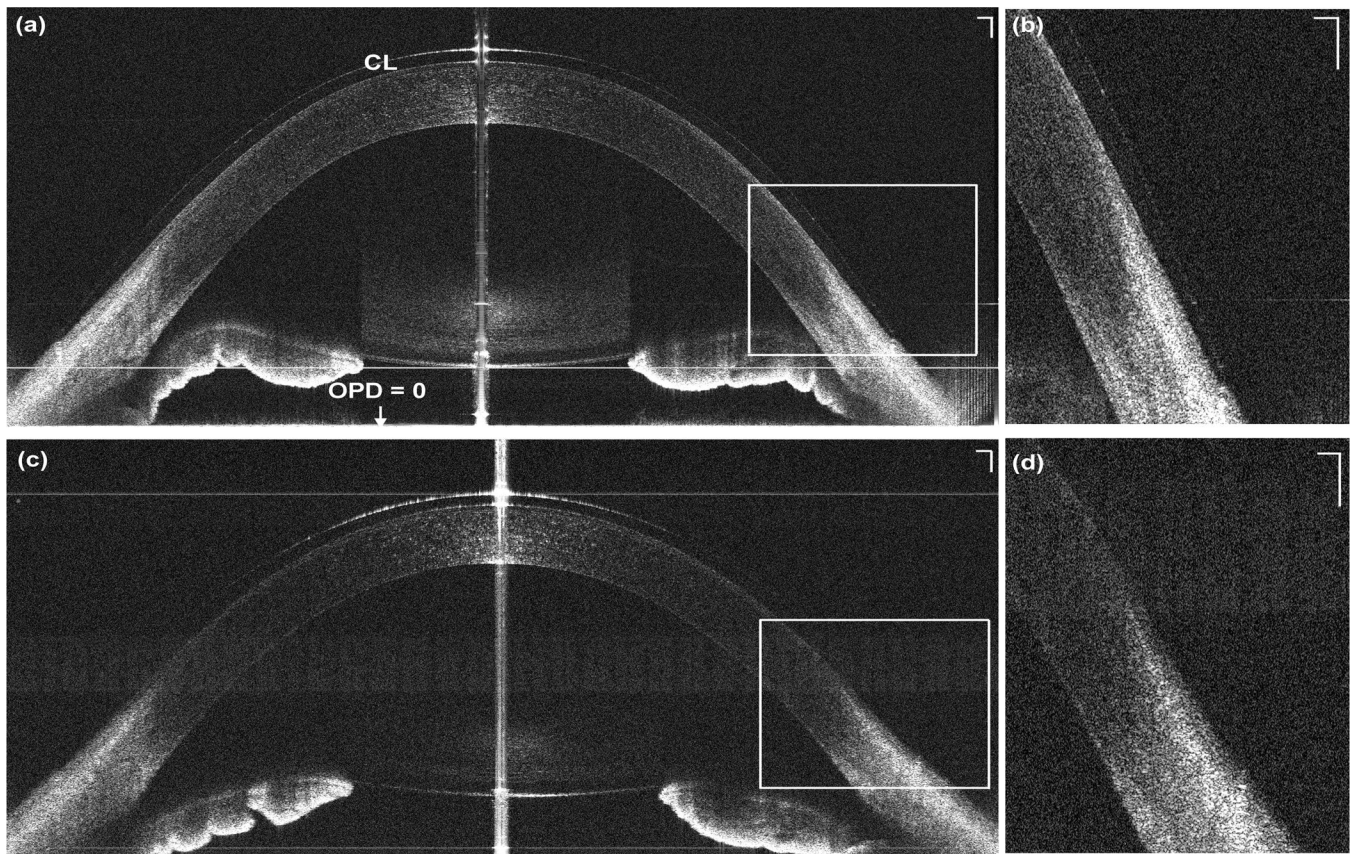


Figure 4. Representative CMOS-based OCT (a) and EX-OCT (c) images of the contact lens in vivo and magnified images of the contact lens edge (b, d)
 The zero delay line (optical path difference $OPD = 0$) is indicated. (a) The entire contact lens on the eye was clearly visualized with the CMOS-based OCT system. (c) The periphery of the contact lens was not clear in the EX-OCT system. CL: contact lens. Bars = 250 μm .
 Note: the crystalline lens and iris was flipped due to the conjugate artifact.

Table 1

Topographic thicknesses (μm) of the epithelium (ET), total cornea (CT) and contact lens (CLT) for five eyes of five subjects using CMOS-based OCT.

Location*	ET		CT		CLT	
	Nasal	Temporal	Nasal	Temporal	Nasal	Temporal
L1	51.3 \pm 4.4	51.4 \pm 3.6	547.9 \pm 15.8	547.3 \pm 21.8	102.9 \pm 8.5	103.6 \pm 4.2
L2	49.5 \pm 4.1	51.9 \pm 3.5	560.1 \pm 15.4	561.4 \pm 22.7	112.9 \pm 9.5	113.3 \pm 5.7
L3	52.7 \pm 3.5	51.1 \pm 3.6	590.9 \pm 13.0	590.0 \pm 17.7	129.5 \pm 7.3	131.2 \pm 9.7
L4	57.3 \pm 5.9	55.6 \pm 7.0	635.3 \pm 16.2	637.0 \pm 13.8	159.5 \pm 7.5	164.6 \pm 11.1
L5	62.7 \pm 6.3	64.7 \pm 5.3	707.7 \pm 22.4	706.8 \pm 20.1	181.1 \pm 8.0	179.0 \pm 5.8
L6	-	-	-	-	148.9 \pm 7.9	140.7 \pm 14.5

* L1, L2, L3, L4, L5, and L6 are chord distances of 1, 2, 3, 4, 5, and 6 mm from the corneal apex, respectively.

Table 2

Repeatability (standard deviation of the difference between two measurements, μm) of CMOS-based OCT to measure the epithelial thickness (ET) and contact lens thickness (CLT) ($n = 5$ eyes).

Location*	ET		CLT	
	Nasal	Temporal	Nasal	Temporal
L1	2.8	1.5	4.0	2.8
L2	3.0	2.4	4.8	5.3
L3	1.9	2.3	9.5	11.1
L4	3.3	3.4	9.5	6.0
L5	3.7	4.1	8.1	8.4
L6	-	-	11.0	10.5

* L1, L2, L3, L4, L5, and L6 are chord distances of 1, 2, 3, 4, 5, and 6 mm from the corneal apex, respectively.